# Real-time System for Nonlinear Load Analysis in 50A Current Range

Marko Dimitrijević, Dejan Stevanović and Miona Andrejević-Stošović

*Abstract* – In this paper we will present 50A current range extension of the system for nonlinear load analysis based on virtual instrumentation paradigm. The presented system is capable of real-time operation, allowing measurements of various parameters, including *THD*, total power factor and various definitions of reactive and distortion power. The system is aimed for three-phase measurements, up to 50A. It is suitable for measurements of multiple small loads connected to one power source (one phase), the common case in households and offices.

*Keywords* – virtual instrumentation, real-time operation, extended current range

## I. Introduction

Power quality analysis of electrical loads is related to measurement of power factor, distortion power and total harmonic distortion. In circuits consisting of linear loads, the currents and voltages are sinusoidal and the power factor effect depends only from the difference in phase between the current and voltage waveforms. In single phase system it is referred to as the displacement power factor or cos(φ) [1]. The power concepts developed for single-phase circuits with sinusoidal voltages and currents can be extended to polyphase circuits. Such circuits can be considered to be divided into a group of two-wire sets, with the neutral conductor (or a resistively derived neutral for the case of a delta-connected, three wire circuit) paired with each other conductor [2].

In the case nonlinear loads are present we should introduce new quantities in the calculations emanated by the harmonics and related power components [3]. Now the power factor can be generalized to a total or true power factor where the apparent power, involved in its calculations, includes all harmonic components. This is of importance in characterization and design of practical power systems which contain non-linear loads such as switched-mode power supplies [4].

The presented system represents extension of previously described system, presented in PhD thesis [5] and our previous papers [6].

Marko Dimitrijević and Miona Andrejević-Stošović are with the University of Niš, Faculty of Electronic Engineering, Aleksandra Medvedeva 14, 18000 Niš, Serbia. Email: {marko.dimitrijevic, miona.andrejevic}@elfak.ni.ac.rs.

Dejan Stevanović is with ICNT, Bulevar Nikole Tesle 61, 18000 Niš, Serbia. E-mail: dejan.stevanovic@icnt.rs.

The extension of system's measuring range is necessary for the analysis of loads with higher nominal power, as well as for the use of non-invasive load monitoring algorithms (NILM), which are applied to a group of loads connected to the same power source (phase) [7-10]. The system consists of an acquisition subsystem and a virtual instrument for calculating parameters and presenting the measurement results.

The system is based on virtual instrumentation paradigm, augmented with real-time component, ensuring determinism in measurement. The system hardware is implemented on field programming gate array (FPGA), it is in control of data acquisition. The system software has two components: application executing on real-time operating system (RTOS) aimed for basic parameter calculation, and user interface application for data analysis, manipulation and visualization that runs on simple operating system (GPOS). The system implemented in such a manner allows measuring and calculating a number of quantities that characterize loads, unobtainable with classical instruments. It offers many advantages – scalability, open architecture and flexibility: it can be simply extended in functionality – by number of calculated parameters and in the number of measurement channels (i.e. phases). It can be employed as a subsystem in harmonic compensation system [11] or used in power-in-the-loop and hardware-in-the-loop applications.

Flexibility is achieved through implementations on different platforms and through usage for different purposes: laboratory equipment for real-time operation (controller equipped with PXI-7813R FPGA card and expansion chassis), compact industrial PC for real-time operation (installed on programmable controller – PAC) or portable instrument connected by USB interface.

The paper is organized as follows: in the second section we will present signal acquisition system, third sections describes algorithms for harmonic analysis and parameter calculation, section four presents virtual instrument for data presentation and analysis and fifth section concludes the paper.

## II. Acquisition

Acquisition subsystem consists of connection board with current sensors, acquisition modules and data interface. The layout of connection board is shown in Fig. 1. The function of the circuit is to connect the power source, the system and the load under test. The circuit consists of four Hall current sensors LEM LA-55P [12], which converts the current signal into a voltage. The conversion ratio is 2000A/V.

Hall sensors are chosen due to good linearity and accuracy at low frequencies, especially when measuring the DC current component. The disadvantage of Hall sensors, compared to the current transformer, is the necessity for external DC power supply.

Current sensor outputs are connected to *National Instruments* NI9215 [13] acquisition module. The acquisition module has four input channels for simultaneous voltage sampling with 16-bit resolution, 100kS acquisition rate and 250$V_{RMS}$ isolation between the acquisition channel and the mass. The NI9215 acquisition module is isolated.

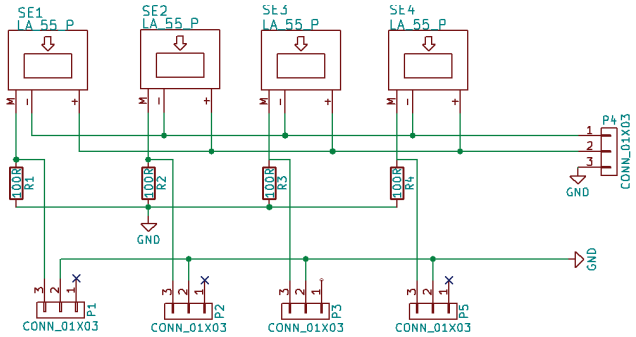


Fig. 1 Connection circuit diagram. The outputs of the LEM LA-55P sensors are connected to the NI9215 acquisition module

The voltage acquisition is implemented directly by connecting the *National Instruments* NI9225 [14] acquisition module. The resolution of the A/D conversion is 24-bit and the sampling rate is 50kS/s. The maximum isolation voltage between the acquisition channel and the ground is 600$V_{RMS}$. The measurement range is 300$V_{RMS}$. The voltage source is connected differentially. The input impedance of each channel is 1 MΩ. Detailed information regarding acquisition modules are given in Table 1.

TABLE I

INPUT CHARACTERISTICS NI 9225 AND NI 9215 MODULES

| Parameter | | NI9225 | NI9215 |
|---|---|---|---|
| Channels | | 3 | 4 |
| Resolution | | 24 | 16 |
| Sampling rate (kS/s) | min | 1.613 | 1.613 |
| | max | 50 | 100 |
| | range | 50/n n=1,2,…,31 | 100/n n=1,2,…,31 |
| Master time base | $f_M$ | 12.8 | 12.8 |
| | Accuracy | ±100ppm | ±100ppm |
| Impedance | | 1 MΩ | 1 GΩ |
| Noise (50kS/s) | | 2.2 mV | 0.18 mV |
| Scaling coefficient | | 50.66 µV/LSB | 305.18 µV/LSB |

The input signals are conditioned, filtered and connected to the input of a 24-bit (16-bit for NI9215) sigma-delta A/D converters. The channels are completely independent and isolated, allowing simultaneous acquisition of three voltage and four current signals.

The sigma-delta A/D converter consists of an integrator, a comparator, a one-bit digital-to-analog converter (DAC) connected in a negative feedback loop and a decimation filter. The output signal of the integrator is compared in a comparator with a reference signal, which produces one bit. The sampling rate $f_{OS}$ is 256 times the minimum frequency defined by the Shannon-Nyquist criterion. A series of bits from the comparator output is fed to the decimation filter input, which average and decimate the signal, giving a 24-bit digital signal with rate $f_S$. The decimation filter has a low-pass filter function, which reduces the quantization noise and aliasing. The decimator is realized as a FIR filter with a cutoff frequency equal to 0.47$f_S$. The bandwidth of the entire acquisition channel is shown in Fig. 2.

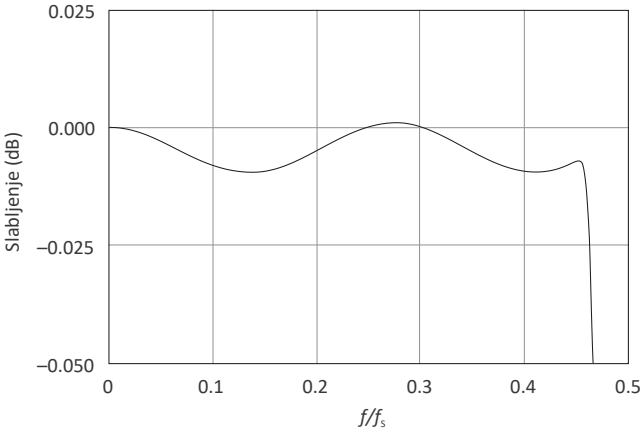


Fig. 2. Channel bandwidth

Sigma-Delta ADC uses an internal time base (Master Time Base) whose frequency is $f_M$=12.8 MHz. The time base can be synchronized with other acquisition modules, thus achieving synchronized sampling of different signals and minimal jitter. Oversampling frequency $f_{OS}$ can be selected depending on the required sampling rate in such way the digital signal at the output of the decimation filter $X_n$ has rate

$$f_S = \frac{f_M}{256 \cdot n}, \quad n = 1,2,...,31. \tag{1}$$

In this implementation the internal time base without dividers is used as oversampling frequency for all acquisition modules. The output digital signal of the ADC is 50kS/s, which corresponds to the bandwidth of the 25kHz input signal. Sigma-Delta ADC, using the oversampling method of acquisition, has several advantages, such as effectively eliminating alliances.

## III. HARMONIC ANALYSIS AND PARAMETER CALCULATION

### *A. Definitions*

We will first introduce the basic definitions that are expressing how the measured quantities are calculated from the current and voltage waveforms according to IEEE Std 1459-2000 [15] and IEEE Std. 1459-2010 [16] standards.

In the presence of nonlinear loads, the system no longer operates in sinusoidal condition and use of fundamental frequency analysis does not apply any more. Traditional power system quantities such as effective value, power (active, reactive, apparent), and power factor need to be numerically calculated from sampled voltage and current sequences by performing DFT or FFT algorithm.

The RMS value of some periodic physical entity $X$ (voltage or current) is calculated according to the well-known formula:

$$X_{\mathrm{RMS}} = \sqrt{\frac{1}{\mathrm{T}} \int_{t_0}^{t_0+\mathrm{T}} \left(x(t)\right)^2 dt} \tag{2}$$

where $x(t)$ represents time evolution, $T$ is the period and $t_0$ is arbitrary time. For any periodic physical entity $x(t)$, we can give Fourier representation:

$$x(t) = a_0 + \sum_{k=1}^{+\infty} \left( a_k \cdot \cos\left(k\omega t\right) + b_k \cdot \sin\left(k\omega t\right) \right) \tag{3}$$

or

$$x(t) = c_0 + \sum_{k=1}^{+\infty} c_k \cdot \cos\left(k\omega t + \psi_k\right) \tag{4}$$

where $c_0 = a_0$ represents DC component, $c_k = \sqrt{a_k^2 + b_k^2}$ magnitude of $k^{\mathrm{th}}$ harmonic, $\psi_k = \arctan\dfrac{b_k}{a_k}$ phase of the $k^{\mathrm{th}}$ harmonic and $\omega = \dfrac{2\pi}{\mathrm{T}}$, angular frequency.

Fourier coefficients $a_k$, $b_k$ are:

$$a_0 = \frac{1}{\mathrm{T}} \int_{-\mathrm{T}/2}^{+\mathrm{T}/2} x(t)dt, \quad a_k = \frac{2}{\mathrm{T}} \int_{-\mathrm{T}/2}^{+\mathrm{T}/2} x(t) \cdot \cos\left(\frac{2k\pi t}{\mathrm{T}}\right) dt \tag{5}$$

and

$$b_k = \frac{2}{T} \int_{-\mathrm{T}/2}^{+\mathrm{T}/2} x(t) \cdot \sin\left(\frac{2k\pi t}{\mathrm{T}}\right) dt. \tag{6}$$

The RMS value of $k^{\mathrm{th}}$ harmonic is

$$X_{\mathrm{k,\,RMS}} = c_k \Big/ \sqrt{2}. \tag{7}$$

We can calculate total RMS value

$$X_{\mathrm{RMS}} = \sqrt{\sum_{k=1}^{M} X_{k,\,\mathrm{RMS}}^2} = \sqrt{X_{\mathrm{1,\,RMS}}^2 + X_{\mathrm{H,\,RMS}}^2} \tag{8}$$

where $M$ is highest order harmonic taken into calculation. Index "1" denotes first or fundamental harmonic, and index "H" denotes contributions of higher harmonics.

Equations (2) – (8) need to be rewritten for voltage and current. Practically, we operate with sampled values and integrals (5) and (6) are transformed into finite sums.

For a single-phase system where $k$ is the harmonic number, $\varphi_k$ phase difference between voltage and current of $k^{\mathrm{th}}$ harmonic and $M$ is the highest harmonic, the total active power is given by:

$$P = \sum_{k=1}^{M} I_{k,\mathrm{RMS}} \cdot V_{k,\mathrm{RMS}} \cdot \cos\varphi_k = P_1 + P_{\mathrm{H}}. \tag{9}$$

The first addend in the sum (9), denoted with $P_1$, is fundamental active power. The rest of the sum, denoted with $P_{\mathrm{H}}$, is harmonic active power.

Total reactive power is given by:

$$Q = \sum_{k=1}^{M} I_{k,\mathrm{RMS}} \cdot V_{k,\mathrm{RMS}} \cdot \sin\varphi_k = Q_1 + Q_H. \tag{10}$$

It should be noted that the actual contribution of harmonic frequencies to active and reactive power is small (usually less than 3% of the total active or reactive power). The major contribution of higher harmonic to the power comes as distortion power $D$:

$$D^2 = \sum_{\substack{j \neq k \\ j=1,k=1}}^{M} I^2_{\,j,\mathrm{RMS}} \cdot V^2_{\,k,\mathrm{RMS}} \tag{11}$$

The apparent power can be written:

$$\begin{aligned} S^2 = &\underbrace{I^2_{\,1,\mathrm{RMS}} \cdot V^2_{\,1,\mathrm{RMS}}}_{S_1^2} + \underbrace{I^2_{\,1,\mathrm{RMS}} \cdot V^2_{\,\mathrm{H,RMS}}}_{D_V^2} + \\ &+ \underbrace{V^2_{\,1,\mathrm{RMS}} \cdot I^2_{\,\mathrm{H,RMS}}}_{D_I^2} + \underbrace{V^2_{\,H,\mathrm{RMS}} \cdot I^2_{\,\mathrm{H,RMS}}}_{S_{\mathrm{H}}^2} \end{aligned} \tag{12}$$

where $S_1$ represents fundamental apparent power, $D_V$ voltage distortion power, $D_I$ current distortion power and $S_{\mathrm{H}}$ harmonic apparent power. $S_1$ and $S_{\mathrm{H}}$ are

$$S_1 = \sqrt{P_1^2 + Q_1^2},\ S_{\mathrm{H}} = \sqrt{P_{\mathrm{H}}^2 + Q_{\mathrm{H}}^2 + D_{\mathrm{H}}^2} \tag{13}$$

where $D_{\mathrm{H}}$ represents harmonic distortion power. The total apparent power is

$$S = \sqrt{P^2 + Q^2 + D^2}. \tag{14}$$

The total harmonic distortions, $THD$, are calculated from the following formula:

$$THD_I = \frac{I_{\mathrm{H,\,RMS}}}{I_{\mathrm{1,\,RMS}}} = \frac{1}{I_{\mathrm{1,\,RMS}}} \sqrt{\sum_{j=2}^{M} I_{j,\,\mathrm{RMS}}^2} = \sqrt{\frac{I_{\mathrm{RMS}}^2 - I^2_{\,\mathrm{1,\,RMS}}}{I^2_{\,\mathrm{1,\,RMS}}}} \tag{15}$$

and

$$THD_V = \frac{V_{\mathrm{H},RMS}}{V_{\mathrm{1},RMS}} = \frac{1}{V_{\mathrm{1},RMS}} \sqrt{\sum_{k=2}^{M} V_{k,\,\mathrm{RMS}}^2} = \sqrt{\frac{V_{\mathrm{RMS}}^2 - V^2_{\,\mathrm{1,\,RMS}}}{V^2_{\,\mathrm{1,\,RMS}}}} \tag{16}$$

where $I_j$,$V_k$ $j$,$k$=1, 2, …, $M$ stands for the harmonic of the current or voltage. It can be shown that:

$$\begin{aligned} D_I &= V_{1,\,\mathrm{RMS}} \cdot I_{\mathrm{H,\,RMS}} = S_1 \cdot THD_I \\ D_V &= V_{\mathrm{H,\,RMS}} \cdot I_{1,\,\mathrm{RMS}} = S_1 \cdot THD_V \\ S_H &= S_1 \cdot THD_I \cdot THD_V . \end{aligned} \tag{17}$$

Fundamental power factor or displacement power factor is given by the following formula:

$$PF_1 = \frac{P_1}{S_1} = \cos\varphi_1 . \tag{18}$$

Total power factor *DPF*, taking into calculation (9) and (12), is

$$TPF = \frac{P}{S} = \frac{P_1 + P_\mathrm{H}}{\sqrt{S_1^2 + D_I^2 + D_V^2 + S_\mathrm{H}^2}} \tag{19}$$

and substituting (17) and (18):

$$TPF = \frac{\left(1 + \dfrac{P_\mathrm{H}}{P_1}\right)\cos\varphi_1}{\sqrt{1 + THD_I^2 + THD_V^2 + \left(THD_I THD_V\right)^2}} \tag{20}$$

In real circuits, $P_\mathrm{H} << P_1$ and voltage is almost sinusoidal ($THD_V$<5%), leading to simpler equation for *TPF*:

$$TPF = \frac{\cos\varphi_1}{\sqrt{1 + THD_I^2}} . \tag{21}$$

*B. Harmonic analysis implementation*

Frequency analysis of the signal is realized in two ways: in hardware, using the FPGA (*Field Programming Gate Array*) when the system is operating in real time, and in software when time determinism is not crucial point.

The function of the FPGA circuit is the determination of the fundamental frequency and the harmonic analysis of the current and voltage waveforms, i.e. calculation of harmonic amplitudes and phases. Algorithms are implemented on the Xilinx Vitex-II FPGA integrated circuit. FPGA is placed on the National Instruments PXI-7813R card connected to the NI-8014 PXI controller, via PCI interface [17]. The FPGA circuit clock is 40MHz. The card has 160 bidirectional digital channels, which support 3.3 V, 5 V, LVTTL and TTL logic levels. It supports 160 64-bit resolution and 40 MHz frequencies, with a maximum error of 100ppm. The card has 196 KB of memory, and the total number of DMA channels is 3.

Bidirectional channels are aggregated into four groups, each representing a separate physical connector. Through one 40-bit connector, the NI9151 extension housing, which includes the NI9225 and NI9215 acquisition modules is connected to the card. FPGA is connected to the PXI controller via PCI bus.

The FPGA circuit performs three parallel processes. The function of the first process is to control the acquisition of the signal. The process is performed in a programming loop that is repeated at time intervals equal to the integer duration of the cycle of the clock. The sampling rate of the signal is equal to the loop repetition frequency for acquisition.

The second process performs harmonic analysis of the selected signals using Goertzel algorithm [18]. The iterative part of the algorithm is executed on a block of 2000 samples, which at the maximum sampling speed corresponds to 40ms in time domain. The real and imaginary part of the spectrum are calculated in the non-iterative part of the algorithm:

$$\begin{aligned} \mathrm{Re}\left(X_k\right) &= S_k^{(\mathrm{N}-1)} - S_k^{(\mathrm{N}-2)} \cdot \cos\left(\frac{2\pi k}{\mathrm{N}}\right) \\ \mathrm{Im}\left(X_k\right) &= S_k^{(\mathrm{N}-2)} \cdot \sin\left(\frac{2\pi k}{\mathrm{N}}\right). \end{aligned} \tag{22}$$

Values for $\sin\left(\frac{2\pi k}{\mathrm{N}}\right)$ and $\cos\left(\frac{2\pi k}{\mathrm{N}}\right)$ are stored in the block memory (lookup table).

The function of the third process is transferring data from the FPGA to the data processing subsystem. The transfer takes place over three 64-bit DMA channels. In one process cycle, 192 bits can be transferred.

In the case of software-implemented frequency analysis, acquisition modules are connected via National Instruments cDAQ-9174 chassis and USB interface to a computer. sampled values of current and voltage are transmitted via the DAQmx driver to a virtual instrument for further analysis. Frequency analysis is performed using standard algorithms, available as LabVIEW modules [19]. These functions can be implemented on a real-time operating system [20] or a general-purpose operating system.

*C. Parameter calculation*

The software component of the system is implemented using National Instruments LabVIEW development package, which provides the possibility of simple realization of virtual instruments [21]. The virtual instrument consists of an interface to the acquisition module, a procedure for calculating numerical values and a user interface.

The interface to the acquisition modules is implemented through the DAQmx driver. Physical channels are represented as virtual channels. A virtual channel is a set of attributes assigned to a specific measurement and includes the name of the channel, the physical channel through which the measurement is performed, the inbound connection terminals, the type of measurement and scaling. The physical channel determines the terminal on the acquisition module to which the receiving signal is fed. A virtual channel can be configured globally at the system level, or locally in the application itself through an application interface. Each physical channel has a unique name.

It is possible to aggregate multiple virtual channels that define the same types of measurements in one measurement process. Processes, similar to virtual channels, can be defined locally at the application level and globally at the system level.

The application implemented using LabVIEW

developing package consists of three threads, exploiting contemporary multicore capabilities. First thread receives data from FPGA level. Second thread calculates power quantities: apparent power, active power, reactive power and energy; power quality parameters including total harmonic distortion ($THD_I$, $THD_V$), crest factors, total power factor and displacement power factor. Third thread handles TCP/IP communication with user interface.

The application is capable of logging measured values and calculated parameters and events locally on a hard disk drive (Fig. 3). All measured and calculated parameters, transient analysis, as well as triggered events are stored on hard disk or other type of data storage. The data quantity and therefore the measurement time, depends on the storage capacity. A separate thread is responsible for network communication with the user PC.

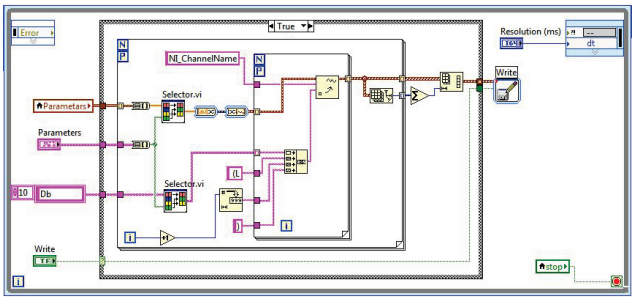


Figure 3. A part of the real-time application

## IV. Virtual Instrument

The user interface virtual instrument is implemented in National Instruments LabVIEW developing package, which provides for simple creation of virtual instruments [21]. The virtual instrument is an application running on general purpose operating system (GPOS) such as Microsoft Windows, Linux or MacOS, connected with RTOS over the network. It consists of an interface to real-time application and a graphic user interface. The communication between the user interface and the real-time application is implemented using TCP/IP protocol.

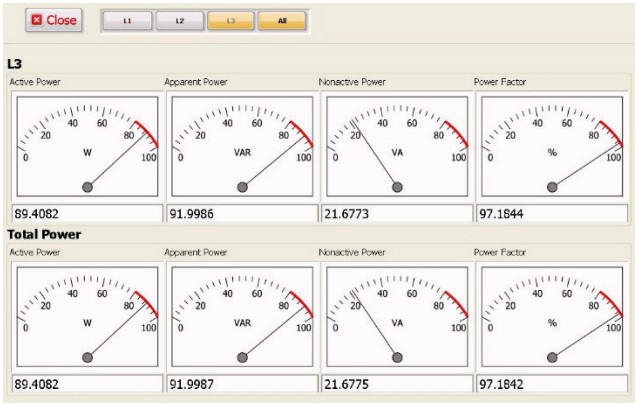


Fig. 4. Virtual instrument graphic interface displaying active, apparent and non-active power, as well as power factor for L3 phase and all phases

The user interface of the virtual instrument consists of visual indicators. It provides basic functions for measurement. The indicators – gauges and graphs – show measured values. User interface also provides controls for data manipulation and saving the measured values (Fig. 4).

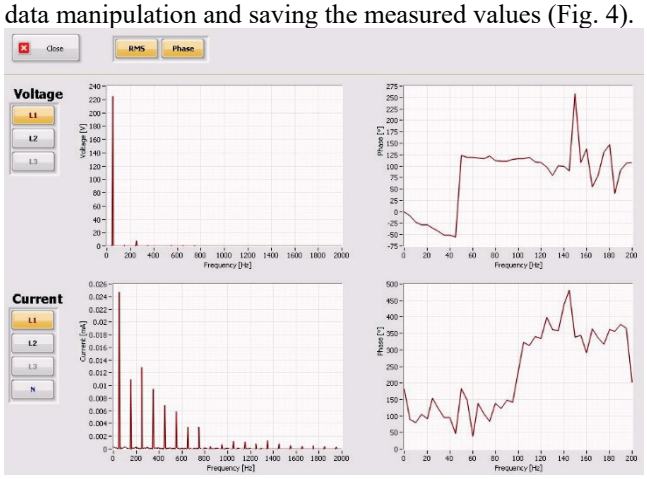


Fig. 5. Virtual instrument shows voltage and current spectra for L1 phase

The virtual instrument shows waveforms and spectra of measured voltages and currents (Fig. 5 and 6). Measured electrical quantities such as RMS and DC values, as well as calculated power quantities are shown in the front panel using virtual gauges and numeric indicators. Power factor and other power quality parameters are shown numerically. The virtual instrument can operate in one phase or three phase mode.

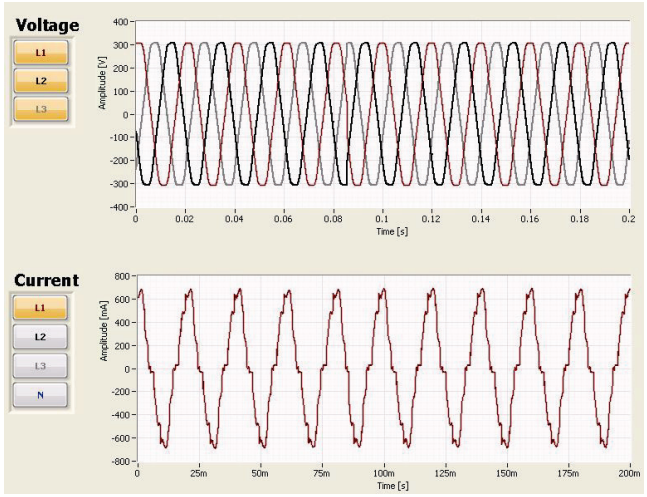


**Fig. 6. Voltage waveforms for all phases, current waveform of L1**

Harmonic magnitudes are shown in a table and each magnitude can be represented separately.

## IV. Conclusion

A new approach to power factor and distortion analysis in polyphase systems was presented. It aggregates the

advantages of virtual instrumentation and the real-time response of classical instruments, capable for real-time sampling and measuring voltage and current of the device under test, providing possibility for transient analysis in time and frequency domain. FPGA and RTOS are taking the main role in data processing of all kind. In this way we introduced a flexible and versatile system with practically unlimited possibilities. The network PC has the control and user interface function.

The system elaborated in this paper is implemented as laboratory instrument using PXI-8105 controller running PharLap OS, equipped with PXI-7813R Virtex-II 3M gate FPGA programmable card and cRIO-9151 expansion chassis. Alternatively, it can be realized using programmable automation controllers (PAC) such National Instruments CompactRIO series. The small sized CompactRIO system includes acquisition modules, FPGA chassis and a real-time controller running VXWorks RTOS. It is suitable for long time executions and hard-ware-in-the-loop tests.

The presented application is capable for three-phase operation. However, the system is exceedingly scalable – it can be easily extended by adding additional acquisition modules into the expansion chassis.

## ACKNOWLEDGEMENT

This research was partly funded by The Ministry of Education and Science of Republic of Serbia under contract No. TR32004.

## REFERENCES

[1] H. W. Beaty, D. G. Fink, *Standard handbook for electrical engineers* (McGraw-Hill, New York, 2007).

[2] John G. Webster, *The Measurement Instrumentation and Sensors Handbook* (CRC Press, 1999).

[3] T. H. Tumiran, M. Dultudes, *"The Effect of Harmonic Distortion to Power Factor"*, Proceedings of the International Conference on Electrical Engineering and Informatics, 2007, pp. 834–837 Institute Teknologi Bandung, Indonesia

[4] G. Moschopoulos, *Single-Phase Single-Stage Power-Factor-Corrected Converter Topologies*, IEEE Trans. on Industrial Electronics 52, 2005, pp. 23–35.

[5] M. Dimitrijević, *Elektronski sistem za analizu polifaznih opterećenja baziran na FPGA*, PhD Thesis, Faculty of Electronic Engineering, University of Niš, Niš, Serbia, 2012.

[6] M. A. Dimitrijević, V. B. Litovski, *Power Factor and Distortion Measuring for Small Loads Using USB Acquisition Module*, Journal of Circuits, Systems, and Computers (JCSC), Vol. 20, No. 5, August 2011

[7] M. Andrejević-Stošović, M. Dimitrijević, D. Stevanović, *"Application of ELM Algorithm in Characterization of Nonlinear Loads"*, Proc. of the 2nd IcETRAN conference, pp. EL1-EL4 Kladovo, 2017

[8] M. Andrejević-Stošović, D. Stevanović, M. Dimitrijević, *"Monitoring and Classification of Nonlinear Loads Based on Artificial Neural Networks"*, 13th International Conference on Advanced Technologies, Systems and Services in Telecommunications (TELSIKS), Niš, 978-1-5386-1799-1, doi: 10.1109/TELSKS.2017.8246320

[9] M. Andrejević-Stošović, D. Stevanović, M. Dimitrijević, *"Classification of Nonlinear Loads Based on Artificial Neural Networks"*, IEEE 30th International Conference on Microelectronics (MIEL), Niš, 978-1-5386-2561-3, doi:10.1109/MIEL.2017.8190107

[10] Djordjević, S., Dimitrijević, M., Litovski, V., A Non-Intrusive Identification of Home Appliances Using Active Power and Harmonic Current, Facta Universitatis, Series: Electronics and Energetics, Vol 30, No 2, Niš, ISSN 0353-3670, doi: 10.2298 /FUEE1702199D

[11] M. Dimitrijević, D. Stevanović, M. Andrejević Stošović, M. Petronijević, P. Petković, *"Compensation of Harmonics in Smart Grid Using Photovoltaic Energy Source"*, XI International Symposium on Industrial Electronics - INDEL 2016, Banja Luka, 03.11.-05.11. 2016, pp. 1-6.

[12] LEM: Current Transducer LA 55-P/SP1 Datasheet

[13] National Instruments: NI 9215 Operating Instructions and Specifications.

[14] National Instruments: NI 9225 Operating Instructions and Specifications.

[15] IEEE Std 1459-2000 – Standard Definitons for the Measurement of Electric Power Quantities Under Sinusoidal, Nonsinusoidal, Balanced or Unbalanced Conditions (The Institute of Electrical and Electronics Engineers, 2000).

[16] IEEE Std 1459-2010 – Revision Standard Definition for the Measurement of Electric Power Quantities Under Sinusoidal, Nonsinusoidal, Balanced or Unbalanced Conditions (The Institute of Electrical and Electronics Engineers, 2010).

[17] National Instruments: NI PXI-7813R R Series Digital RIO with Virtex-II 3M Gate FPGA.

[18] Goertzel, G.: *"An Algorithm for the Evaluation of Finite Trigonometric Series."* The American Mathematical Monthly, January 1958, No. 1, Vol. 65, pp. 34-35.

[19] National Instruments: NI PXI-7813R R Series Digital RIO with Virtex-II 3M Gate FPGA.

[20] Jarvis, C., Kinsella, K., Timpanaro, P.: *"Phar Lap ETS™ – An Industrial-Strength RTOS White Paper."*

[21] National Instruments: LabVIEW System Design Software.